

MathDoc: Benchmarking Structured Extraction and Active Refusal on Noisy Mathematics Exam Papers

Chenyue Zhou⁵, Jiayi Tuo⁶, Shitong Qin², Wei Dai³, Mingxuan Wang¹,
 Ziwei Zhao¹, Duoyang Li¹, Shiyang Su¹, Yanxi Lu¹, Yanbiao Ma^{1,3,4*}

¹Gaoling School of Artificial Intelligence, Renmin University of China Beijing, China

²Gaotu Techedu Inc. ³Beijing Key Laboratory of Research on Large Models and Intelligent Governance

⁴Engineering Research Center of Next-Generation Intelligent Search and Recommendation, MOE

⁵Nanjing University of Aeronautics and Astronautics

⁶University of Science and Technology of China

Abstract

The automated extraction of structured questions from paper-based mathematics exams is fundamental to intelligent education, yet remains challenging in real-world settings due to severe visual noise. Existing benchmarks mainly focus on clean documents or generic layout analysis, overlooking both the structural integrity of mathematical problems and the ability of models to actively reject incomplete inputs. We introduce MathDoc, the first benchmark for document-level information extraction from authentic high school mathematics exam papers. MathDoc contains **3,609** carefully curated questions with real-world artifacts and explicitly includes unrecognizable samples to evaluate active refusal behavior. We propose a multi-dimensional evaluation framework covering stem accuracy, visual similarity, and refusal capability. Experiments on SOTA MLLMs, including Qwen3-VL and Gemini-2.5-Pro, show that although end-to-end models achieve strong extraction performance, they consistently fail to refuse illegible inputs, instead producing confident but invalid outputs. These results highlight a critical gap in current MLLMs and establish MathDoc as a benchmark for assessing model reliability under degraded document conditions. Our project repository is available at [GitHub repository](#)

1 Introduction

In modern educational (Hariyanto et al., 2025) scenarios, the complete and accurate extraction of questions from paper-based mathematics examinations into structured databases is a prerequisite for intelligent test assembly and personalized instruction (Yan et al., 2025). Furthermore, constructing high-quality structured question banks provides high-value corpus support for training the mathematical reasoning (Liu et al., 2025b; Chen et al., 2025b,a; Liu et al., 2025a) capabilities of Large

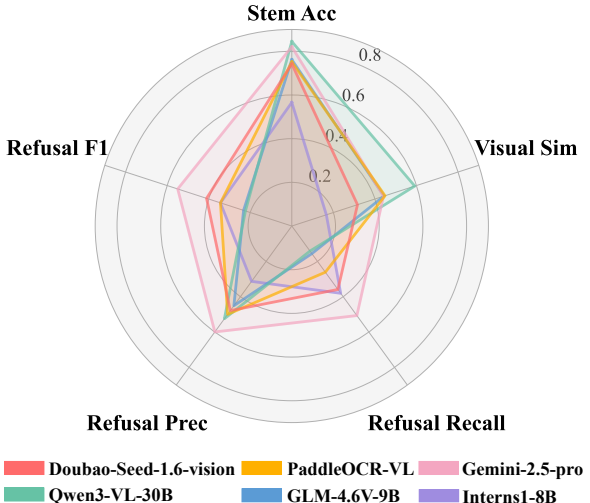


Figure 1: Performance comparison of six Multi-modal Large Language Models (MLLMs) across five metrics (Stem Accuracy, Visual Similarity, Refusal F1/Precision/Recall) in choice questions.

Language Models (LLMs). However, information extraction from examination documents in real-world scenarios faces several critical challenges:

- **Noise Interference:** Handwritten solutions and grading marks frequently overlap with printed text, complicating the extraction of question stems.
- **Figure Extraction:** Flexible layouts complicate text-diagram association, requiring simultaneous localization and contextual alignment.
- **Invalid Information Rejection:** Real-world artifacts (Wang et al., 2025) like creases or occlusions frequently truncate question content. A key challenge lies in enabling models to actively identify and reject such incomplete information.

While the rapid evolution of MLLMs (Zhu et al., 2025; Rasheed et al., 2024; Li et al., 2024; Meng et al., 2024; Bai et al., 2025c; Hu et al., 2024) and the establishment of benchmarks like OCREBench v2 (Fu et al., 2024), OmniDocbench (Ouyang et al.,

*Corresponding author

2025) have jointly advanced general document information extraction, current evaluations remain inadequate for authentic mathematics documents. Data-wise, existing benchmarks prioritize clean documents with standardized layouts, overlooking real-world noise. Task-wise, they operate on the assumption of input completeness, evaluating only extraction correctness while neglecting the critical capability to actively reject incomplete inputs.

To bridge this gap, we introduce MathDoc, a large-scale benchmark of 3,609 high school mathematics questions captured in real educational settings. As is shown in Figure 1, the radar chart illustrates the performance of selected models across different evaluation metrics in choice questions. We conducted comprehensive experiments on both open-source models (Qwen3-VL (Bai et al., 2025b), InternS1 (Bai et al., 2025a), GLM-4.6V, DeepSeek-OCR (Wei et al., 2025), MinerU2.5 (Niu et al., 2025), PaddleOCR-VL (Cui et al., 2025)) and closed-source models (Gemini-2.5-Pro (Comanici et al., 2025), GPT-4o (Hurst et al., 2024), Doubao-Seed-1.6-vision). Our experiments reveal that while SOTA models demonstrate impressive accuracy in extracting content from recognizable samples, they universally struggle with active refusal when facing incomplete or occluded inputs. Instead of acknowledging uncertainty, these models predominantly exhibit a tendency towards speculative completion and forced transcription, highlighting a critical gap in the reliability of current MLLMs for real-world applications.

In summary, the contributions of this paper are summarized as follows:

- We introduce **MathDoc**, the first benchmark for document-level information extraction from real-world high school mathematics exam papers. The benchmark consists of **3,609 high-quality math problems** and establishes a novel **multi-dimensional evaluation protocol** to comprehensively assess a model’s ability in problem statement identification under noisy document conditions, figure extraction, and answer refusal.
- We conduct a systematic evaluation of **SOTA MLLMs**, covering both open-source and close-source models, providing a comprehensive comparison of their performance.
- We conduct a comprehensive analysis to determine the decision boundaries of active refusal

in current MLLMs, quantifying the threshold of information loss to trigger refusal. Furthermore, we propose a simple yet effective method to enhance the refusal capability.

2 Related Works

2.1 General Document Information Extraction Benchmarks

Existing benchmarks (Yang et al., 2025; Heakl et al., 2025; Liu et al., 2024) for document information extraction primarily focus on layout analysis (Zhong et al., 2019; Li et al., 2020a; Zhong et al., 2020) and visual question answering (Zhou et al., 2025; Ma et al., 2024; Mathew et al., 2021; Kim et al., 2019), treating documents as collections of generic layout elements (Jaume et al., 2019) or OCR tokens. However, they fail to assess unit-level structural integrity, which is critical for mathematical parsing. Specifically, current metrics overlook the cohesive extraction of “question units” (integrated stems, options, and figures), leaving a significant gap in evaluating question-level structural parsing (Blecher et al., 2023) capabilities.

2.2 Mathematics Specific Document Information Extraction Benchmarks

Exploration within the specific domain of mathematics document information extraction remains relatively scarce. Existing research falls into two primary categories: one focuses on formula extraction (Horn and Keuper, 2025; Bai et al., 2025d; Li et al., 2020b); the other (Lu et al., 2023; Zhang et al., 2024; Feng et al., 2025; Ye et al., 2025), comprising the majority of recent studies, focuses on mathematical problem-solving capabilities under idealized visual inputs, rather than low-level document restoration capabilities. Crucially, both categories overlook complex document inputs from authentic educational scenarios, resulting in a lack of effective evaluation regarding model extraction performance under noise interference.

3 Dataset Construction

3.1 Data Acquisition

We collected approximately **30,000** raw exam images from real-world high school mathematics scenarios, capturing diverse capture devices and physical conditions. To construct a benchmark that rigorously evaluates model robustness, as is illustrated in Figure 2(a) we curated **460** highly challenging images via a two-stage pipeline:

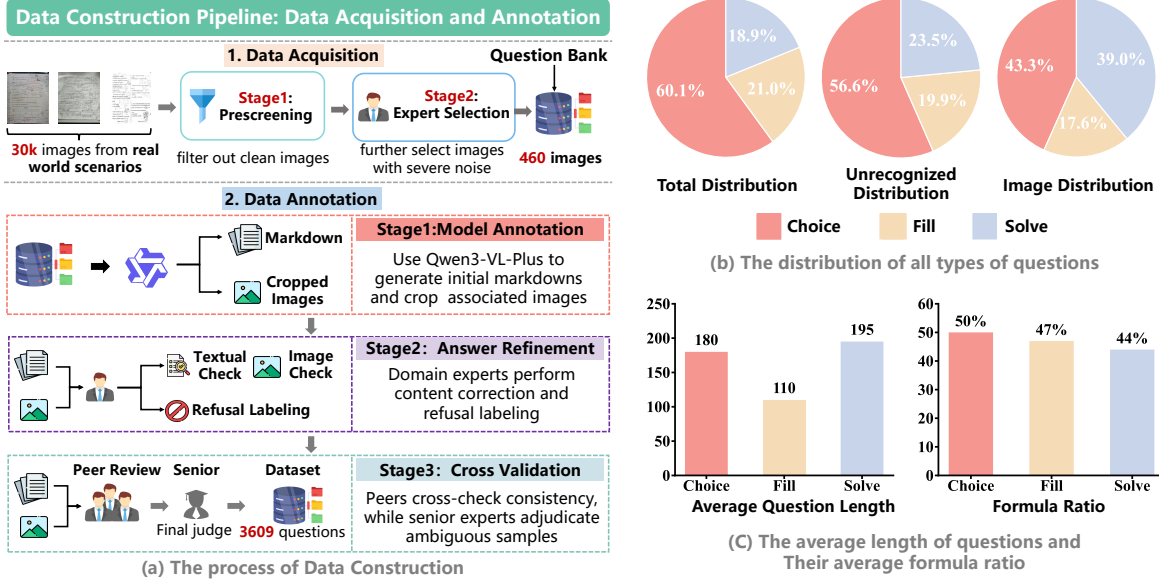


Figure 2: (a) The process of Data Construction. (b) The distribution of all types of questions. (c) The average length of questions and Their average formula ratio.

Layout Pre-screening: We explicitly filter out clean, simple samples to focus on complex geometries. We retain only those featuring multi-column layouts, dense text-figure interleaving to simulate authentic analysis challenges.

Expert Selection: Human experts further identify samples with severe OCR noise, specifically targeting: (1) heavy handwriting occlusions and corrections in critical text regions; (2) physical obstructions (e.g., stains, wrinkles); and (3) compromised document integrity, such as incomplete questions or folded pages.

3.2 Data Annotation

To balance high-quality ground truth with annotation efficiency, as is illustrated in Figure 2(a) we established a standardized three-stage pipeline:

Model-Assisted Pre-annotation: Leveraging the SOTA model Qwen3-VL-Plus, we generate initial structural Markdown sequences and automatically crop associated geometric figures. This provides a high-quality baseline, significantly reducing the manual workload of starting from scratch.

Answer Refinement: Domain experts perform character-level verification under two strict protocols: (1) **Content Correction**, which involves rectifying textual errors and ensuring precise figure cropping; and (2) **Refusal Labeling**, where samples rendered illegible by noise are strictly assigned type-specific placeholders ([Unrecognizable Choice]). This establishes a basis for refusal benchmarking.

Cross-Validation: To eliminate subjective bias, particularly in defining the boundary between “recognizable” and “unrecognizable,” we implement a two-tier quality control mechanism: peer cross-checks (focusing on L^AT_EX syntax and refusal consistency), and a final adjudication by senior experts for ambiguous borderline samples.

3.3 Dataset Properties

As is illustrated in Figure 2(b), the charts present the proportion of Choice, Fill, and Solve questions for overall benchmark and its specific subsets. The first chart represents the overall distribution, which consists of **2,169** Choice, **758** Fill, and **682** Solve questions. The second chart shows the distribution within the subset of questions containing figures, comprising **162** Choice, **66** Fill, and **146** Solve. The third chart depicts the distribution within the “Unrecognizable” subset, which includes **381** Choice, **134** Fill, and **158** Solve.

Regarding content details in Figure 2(c), the average character length per question ranges from **110** to **195**, with Solve questions being the longest. Furthermore, mathematical formulas constitute a substantial portion of the text (ranging from 44% to 50%), requiring models to possess robust capabilities in complex formulation recognition.

4 Benchmark Construction

4.1 Task Definition

We define this task as a document structured extraction problem. Given an input image of a math-

ematics exam paper I , the goal is to parse it and generate a structured set of problems:

$$\mathcal{S} = \{q_1, q_2, \dots, q_N\}. \quad (1)$$

This task requires the model to simultaneously perform three sub-tasks: structured text extraction, figure extraction, and intelligent rejection.

Structured Text Extraction: The extracted problem text T_i must not only match the content in the document exactly, but also preserve the reading order consistent with human perception (top-to-bottom, left-to-right).

Figure Extraction: For problems q_i containing geometric figures, the model is required to predict the bounding box coordinates B_i of the figure, where the corresponding cropped image region must exhibit high semantic similarity with the ground-truth figure.

Intelligent Rejection: Only problems with complete visual information should be extracted. We define a ground-truth-based completeness function

$$\Phi(I, q_i) \in \{0, 1\}. \quad (2)$$

The expected output of the model O_i is:

$$O_i = \begin{cases} T_i, & \text{if } \Phi(I, q_i) = 1 \\ \langle \text{REJECT} \rangle, & \text{if } \Phi(I, q_i) = 0 \end{cases} \quad (3)$$

Here, $\Phi = 0$ (ground-truth rejection) is defined by the following two cases:

- **Critical Occlusion:** The core region of the problem is completely covered.
- **Physical Truncation:** The problem is located at the edge of image, causing semantic interruption.

4.2 Evaluation Pipeline Construction

To provide a fair and comprehensive evaluation of different models, we propose an end-to-end evaluation pipeline, arranged sequentially in the following steps: pre-processing, text matching, rejection matching, and metric computation (see Figure 3).

4.2.1 Pre-Processing

To ensure robust downstream matching, we define a text normalization function $\phi(\cdot)$ that standardizes input sequences through the following operations:

Filtering Non-Semantic Noise: We eliminate irrelevant metadata (exam instructions, headers) using rule-based regex to reduce interference.

Canonicalizing Formats: We reduce ambiguity by unifying L^AT_EX mathematical syntax and converting relative image paths to absolute ones.

Decoupling Reference Answers: We explicitly separate answers from problem statements to accurately confine the downstream matching scope.

4.2.2 Text Matching

This process establishes a fine-grained semantic mapping between valid questions in the Ground Truth (GT) and the model predictions (Pred) by precisely locating question boundaries within the continuous, unstructured prediction stream.

Problem Definition: Given a GT question set $\mathcal{Q} = \{q_i\}_{i=1}^M$ and a Pred text stream \mathcal{T} of length N , the goal is to determine a sequence of boundary indices for precise text matching:

$$\hat{\Omega} = \{[\hat{s}_i, \hat{e}_i]\}_{i=1}^M \quad (4)$$

Here, \hat{s}_i and \hat{e}_i represent the integer character indices in \mathcal{T} , corresponding to the start and end of the i -th question. These indices must satisfy the strict sequential constraint:

$$1 \leq \hat{s}_1 < \hat{e}_1 \leq \hat{s}_2 < \dots < \hat{e}_M \leq N \quad (5)$$

Boundary Indices Localization: To achieve robust alignment, we propose a hierarchical strategy that synergizes semantic understanding with deterministic search. The process operates in two sequential phases: (1) Substring Extraction, extracting text segments based on semantic correspondence; and (2) Index Localization, determining their precise integer indices.

- (1) **Substring Extraction:** This phase utilizes the LLM to identify the specific textual segments that demarcate the boundaries of each question q_i within the noisy prediction stream \mathcal{T} .

$$(\text{str}_i^{\text{start}}, \text{str}_i^{\text{end}}) = \text{LLM}(q_i \mid \mathcal{T}, \mathcal{Q}) \quad (6)$$

By jointly processing the ground-truth question set \mathcal{Q} and the predicted text stream \mathcal{T} , the model locates the start ($\text{str}_i^{\text{start}}$) and end boundary ($\text{str}_i^{\text{end}}$) of each question q_i within the noisy stream \mathcal{T} .

- (2) **Index Localization:** Let k denote a candidate start index in the predicted text stream \mathcal{T} , used to locate either start anchor \hat{s}_i or end anchor \hat{e}_i of question q_i , with the optimal index determined via the following hierarchical search:

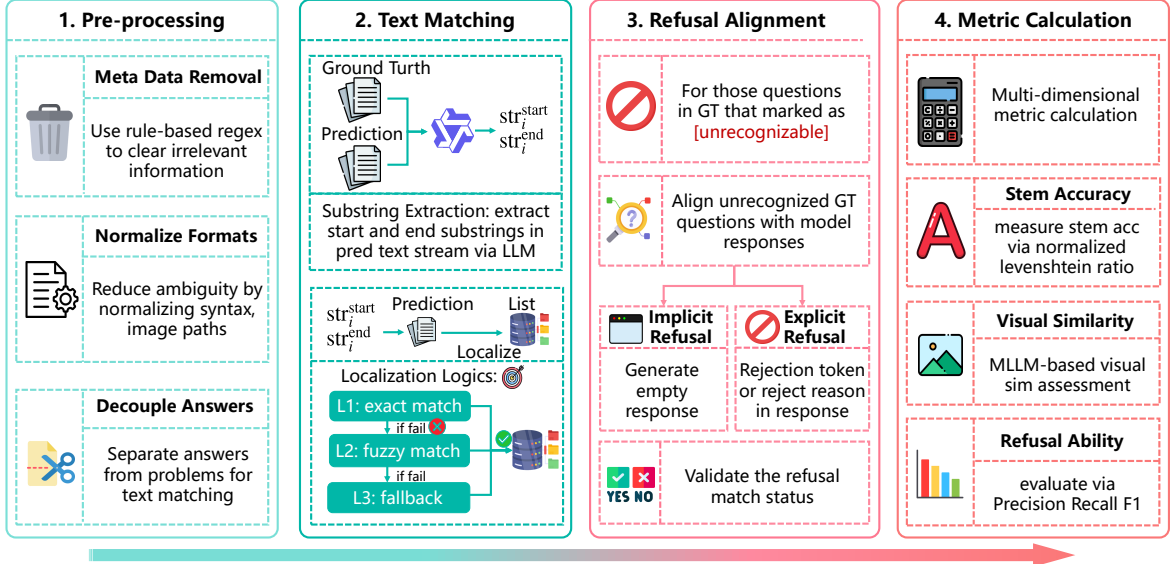


Figure 3: The pipeline of evaluation process

$$\hat{k} = \begin{cases} \text{find}(\text{str} \subset \mathcal{T}), & \text{L1}, \\ \arg \max_k \text{sim}(\text{str}, \mathcal{T}_k), & \text{L2}, \\ k_{\text{fall}}, & \text{L3} \end{cases} \quad (7)$$

Localization Logic: The search logic follows three distinct levels:

- **Level 1 (Exact Match)** Scans the text stream to locate the exact literal occurrence of the anchor substring in pred text streams.
- **Level 2 (Fuzzy Match)** If exact match fails, a sliding window (8–15 characters) traverses the text. The position with the highest normalized Levenshtein similarity is selected, provided the score exceeds the threshold $\tau = 0.8$.
- **Level 3 (Index Fallback)** If both matches fail, the algorithm defaults to the last verified position to maintain continuity. Specifically, it assigns the previous question’s end index to a missing start anchor ($\hat{s}_i \leftarrow \hat{e}_{i-1}$) or collapses a missing end anchor to the current start index ($\hat{e}_i \leftarrow \hat{s}_i$).

4.2.3 Refusal Alignment

For ground truth entries marked as noise (“[Unrecognizable]”), text matching is inapplicable. Instead, we employ a refusal alignment strategy:

- **Implicit Refusal:** The model yields an empty output ($\hat{y}_i = \emptyset$) for a certain question.
- **Explicit Refusal:** The model generates predefined rejection tokens (e.g., “[Unrecognizable]”)

or reasons for refusal to answer, achieving a direct label match with the ground truth.

4.2.4 Evaluation Metrics

We evaluate the model’s performance across three dimensions using the following metrics.

Stem Accuracy: We utilize the Normalized Levenshtein Ratio to quantify the text extraction similarity across all M questions:

$$S_{\text{text}} = \frac{1}{M} \sum_{i=1}^M \left(1 - \frac{\text{Lev}(\phi(T_i^{\text{Pred}}), \phi(Q_i^{\text{GT}}))}{\max(|\phi(T_i^{\text{Pred}})|, |\phi(Q_i^{\text{GT}})|)} \right) \quad (8)$$

Visual Similarity: We employ a MLLM (Qwen3VL-Plus) as a Semantic Judge (Chen et al., 2024) \mathcal{J} to assess the visual similarity between the extracted image I_i^{Pred} and the ground truth I_i^{GT} :

$$S_{\text{img}} = \frac{1}{M} \sum_{i=1}^M \mathcal{J}(I_i^{\text{Pred}}, I_i^{\text{GT}}) \quad (9)$$

where the function \mathcal{J} outputs a semantic similarity score in the range $[0, 1]$.

Refusal Capabilities: We formulate the identification of incomplete questions as a binary classification task, treating Refusal as the positive class. The model’s performance is evaluated using standard Precision, Recall, and F1-Score.

Final Performance Score: The final performance score aggregates text, image, and refusal metrics. Specifically, the refusal dimension is composed of Precision, Recall, and F1-score, each contributing equally to the dimension’s total weight:

$$S_{\text{final}} = \frac{1}{3} S_{\text{text}} + \frac{1}{3} S_{\text{img}} + \frac{1}{9} (P_{\text{ref}} + R_{\text{ref}} + F1_{\text{ref}}) \quad (10)$$

Metric ↓ / Model →	Gemini-2.5-pro	Qwen3vl-30B	Doubao-Seed-1.6-vision	Qwen3vl-8B	Glm-4.6V-9B	Paddleocrvl	Interns1-8B	GPT-4o	Mineru2.5	Deepseek-OCR
Stem	0.8682	0.8891	0.8296	0.8559	0.7843	0.6986	0.6028	0.4951	0.5252	0.3909
Visual	0.4594	0.6267	0.4511	0.4226	0.4887	0.4565	0.1838	0.1967	0.2388	0.2018
Recall	0.5886	0.2038	0.3101	0.2420	0.2903	0.2911	0.2715	0.3333	0.2357	0.3789
Precision	0.7815	0.7805	0.7313	0.6786	0.5625	0.8070	0.2733	0.3490	0.2913	0.2364
F1	0.6715	0.3232	0.4356	0.3568	0.3830	0.4279	0.2724	0.3410	0.2606	0.2912
Final	0.6694	0.6505	0.5910	0.5680	0.5617	0.5546	0.3530	0.3443	0.3422	0.2982

Figure 4: Model performance on Solve, sorted in descending order according to the Final metric (left to right).

5 Experiments

In this section, we benchmark SOTA MLLMs on the **MathDoc** dataset, presenting a comprehensive quantitative evaluation followed by an in-depth analysis. The results are shown in Figure 4, 5 and 6. Furthermore, we design two targeted experiments to investigate the underlying mechanisms of the models’ refusal capabilities. The results are shown in Figure 7 and 8.

5.1 Main Result Analysis

Analysis 1: As shown in Figure 4, Qwen3-VL-30B achieves state-of-the-art extraction performance ($S_{text} = 0.89$, $S_{img} = 0.63$). However, refusal evaluation reveals a consistent ‘‘Low Recall, High Precision’’ pattern across most models (excluding Gemini). For example, despite its strong extraction accuracy, Qwen3-VL-30B attains a refusal recall of only 0.14 (Figure 5). **This imbalance indicates that while models can produce correct refusals when triggered, they rarely initiate refusal proactively.** Instead, they tend to forcibly transcribe fragmented content or speculate missing details. We attribute this behavior to the lack of explicit negative supervision for document incompleteness during pretraining and instruction tuning, resulting in under-trained decision boundaries for completeness-aware rejection.

Analysis 2: Most models perform better on Problem-Solving tasks than on Choice tasks, primarily due to structural differences. Choices require precise localization of densely packed options, where minor spatial misalignment can cause extraction errors. However, Solve tasks provide richer context, enabling models to leverage broader

linguistic priors to mitigate perceptual ambiguities.

Analysis 3: End-to-End MLLMs generally outperform multi-stage pipeline frameworks (MinerU, PaddleOCR-VL). Pipeline approaches typically suffer from error cascading, where failures in the initial layout analysis phase irreversibly corrupt subsequent text recognition.

5.2 Investigation of Refusal Mechanisms

The pervasive low Refusal F1 scores shown in the table necessitate a deeper examination of the underlying refusal behaviors. Consequently, we design targeted experiments to answer two core questions:

- Q1: What degree of information loss triggers a model’s refusal response?
- Q2: What strategies can enhance the model’s refusal performance?

5.2.1 Sensitivity to Information Loss

Experimental Setup: To investigate the specific boundary conditions under which models tend to refuse answering due to missing information, We constructed a evaluation set consisting of 50 independent questions cropped from the original full-page images. To simulate varying degrees of visual incompleteness, we applied a generative erasure technique to all of the images. Specifically, we quantify the extent of information loss based on the textual density within the visual region. We introduce the Information Loss Rate, denoted as η :

$$\eta = \frac{N_{erased}}{N_{total}} \times 100 \quad (11)$$

Consequently, we define the Refusal Rate

Metric ↓ / Model →	Gemini-2.5-pro	Qwen3vl-30B	Paddleocrv1	Glm-4.6V-9B	Doubaos-Seed-1.6-vision	Qwen3vl-8B	Interns1-8B	Deepseek-Ocr	Mineru2.5	GPT-4o
Stem	0.8208	0.8450	0.7518	0.7620	0.7424	0.8237	0.5659	0.4772	0.4742	0.3783
Visual	0.4412	0.5919	0.4487	0.4441	0.3162	0.2844	0.1663	0.2033	0.2394	0.1007
Recall	0.5067	0.1417	0.2613	0.1562	0.3590	0.1530	0.3807	0.3969	0.2619	0.2507
Precision	0.5994	0.5248	0.5000	0.4511	0.4787	0.6042	0.3132	0.2316	0.2129	0.1604
F1	0.5491	0.2232	0.3433	0.2321	0.4103	0.2442	0.3436	0.2925	0.2349	0.1956
Final	0.6045	0.5778	0.5228	0.4952	0.4914	0.4806	0.3592	0.3291	0.3167	0.2271

Figure 5: Model performance on Choice, sorted in descending order according to the Final metric (left to right).

Metric ↓ / Model →	Gemini-2.5-pro	Qwen3vl-30B	Paddleocrv1	Glm-4.6V-9B	Qwen3vl-8B	Doubaos-Seed-1.6-vision	Mineru2.5	Interns1-8B	Deepseek-Ocr	GPT-4o
Stem	0.8346	0.8891	0.7652	0.7454	0.8259	0.7678	0.5335	0.5742	0.4061	0.3618
Visual	0.4277	0.6267	0.4013	0.4094	0.3189	0.3286	0.2673	0.1699	0.1684	0.1237
Recall	0.5338	0.2038	0.3282	0.3819	0.2836	0.3158	0.3813	0.3667	0.4490	0.4286
Precision	0.5820	0.7805	0.6324	0.5000	0.5846	0.4773	0.3272	0.3161	0.2157	0.2262
F1	0.5569	0.3232	0.4322	0.4331	0.3819	0.3801	0.3522	0.3395	0.2914	0.2961
Final	0.6065	0.6505	0.5434	0.5309	0.5205	0.4957	0.3847	0.3615	0.2977	0.2675

Figure 6: Model performance on Fill, sorted in descending order according to the Final metric (left to right).

$R_{ref}(\eta)$ at a specific occlusion level η as:

$$R_{ref}(\eta) = \frac{N_{refused}^{(\eta)}}{N_{set}} \times 100\% \quad (12)$$

where $N_{refused}^{(\eta)}$ denotes the count of **explicitly refused** answers under the occlusion rate η , and N_{set} represents the total number of questions.

Result Analysis: As illustrated in Figure 7, we observe a distinct correlation between model scale and sensitivity to visual occlusion. Taking the 50% refusal rate as a critical threshold, the larger Qwen3VL-30B exhibits the highest sensitivity, identifying and refusing compromised inputs at a low information loss rate of $\eta = 20\%$, followed by GLM at $\eta = 30\%$. In contrast, lightweight models like Interns1-8B and Qwen3VL-8B demonstrate lower awareness of information completeness, attempting to answer even until the occlusion reaches $\eta = 40\%$. This indicates that larger models possess a **superior perception of visual integrity**,

effectively detecting missing contexts to **ensure response reliability**, whereas smaller models are less sensitive to information loss, tending to **process the incomplete visual inputs indiscriminately**.

5.2.2 Exploration on Strategies for Refusal Enhancement

In this subsection, we investigate methods to facilitate the model’s ability to refuse answering when appropriate. Our assumption is that image cropping enhances the model’s visual perception of the specific question. By isolating the question, the model can more easily identify flaws or incompleteness in the visual input, triggering refusal explicitly.

Experimental Setup: We designed a comparative experiment with two input modes:

- In Full-Page Mode, the complete and original test paper image serves as the input. Under this setting, the model exhibits three distinct behaviors: (1) generate an answer, (2) offer no re-

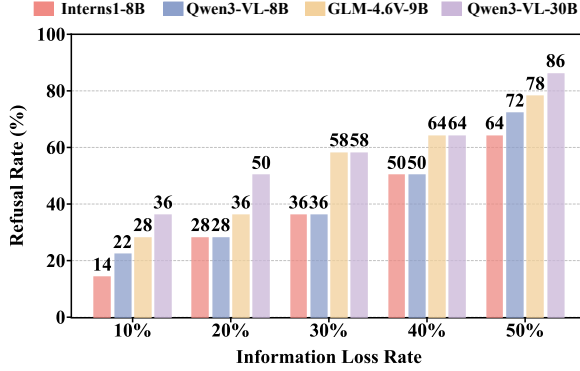


Figure 7: The result of refusal performance.

sponse , or (3) provide an explicit refusal.

- In Single-Question Mode, the specific unrecognizable questions are cropped from the page and input individually. In this scenario, model’s behavior is categorized into two types: (1) generate an answer, or (2) provide an explicit refusal.

To evaluate the effectiveness, we categorize the results based on the joint behavior of the model in both modes. Let $N = 110$ denote the total number of unrecognized questions. We define n_i^j as the number of questions where the model exhibits behavior i in Full-Page , j in Single-Question, where i represents Full-Page behaviors (1: Answer, 2: Silence, 3: Refusal) and j denotes Single-Question behaviors (1: Answer, 2: Refusal).

Based on this notation, we propose three metrics to evaluate the performance:

- Refusal Failure Rate (R_{fail}): This metric measures the proportion of questions where the model persists in generating an answer:

$$R_{fail} = \frac{\sum_{i=1}^3 n_i^1}{N} \quad (13)$$

- Mitigation Rate ($R_{mitigation}$): This metric evaluates the effectiveness of the cropping strategy:

$$R_{mitigation} = \frac{n_1^2 + n_2^2}{N} \quad (14)$$

- Active Refusal Rate (R_{active}): This metric reflects the consistency of the model’s refusal mechanism in both Modes.

$$R_{active} = \frac{n_3^2}{N} \quad (15)$$

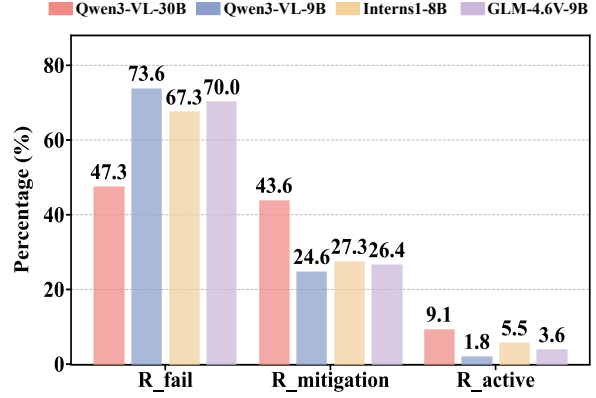


Figure 8: Refusal performance comparison under Full-Page and Single-Question input modes.

Result Analysis: As illustrated in Figure 8, in the full-page mode, models exhibit a significant deficiency in active refusal (R_{active}) (only 1.82% for Qwen3vl-8b) alongside a high failure rate (R_{fail}), indicating a propensity to hallucinate responses rather than decline query. Conversely, upon applying the cropping strategy, we observe a substantial improvement in the models’ ability to refuse incomplete inputs, as evidenced by the mitigation metrics ($R_{mitigation}$). These empirical results strictly validate our assumption: highlighting visual incompleteness through cropping effectively triggers the model’s uncertainty, thereby enabling robust active refusal against incomplete visual contexts.

6 Conclusion

This paper addresses the lack of realistic benchmarks for noisy educational documents by introducing MathDoc, a dataset featuring authentic high school mathematics exams with diverse real-world artifacts and “unrecognizable” samples, along with a comprehensive evaluation framework. MathDoc enables systematic assessments of both information extraction and active refusal capabilities, providing crucial insights for advancing model reliability. Its specific focus on refusal boundaries facilitates targeted model optimization, promoting more faithful and robust Large Language Models.

Limitations

Though we initially explored visual perception enhancement strategies, we have not yet delved into model architecture design or pre-training objective optimization to fundamentally suppress the model’s tendencies for speculative completion and forced transcription in incomplete contexts. Current eval-

uations serve more as a diagnostic tool rather than a generalizable algorithmic solution. Empowering models with the introspective capability to “know what they do not know” remains a critical challenge for building robust document processing systems.

References

Lei Bai, Zhongrui Cai, Yuhang Cao, Maosong Cao, Weihan Cao, Chiyu Chen, Haojiong Chen, Kai Chen, Pengcheng Chen, Ying Chen, Yongkang Chen, Yu Cheng, Pei Chu, Tao Chu, Erfei Cui, Ganqu Cui, Long Cui, Ziyun Cui, Nianchen Deng, and 158 others. 2025a. *Intern-s1: A scientific multimodal foundation model*. *Preprint*, arXiv:2508.15763.

Shuai Bai, Yuxuan Cai, Ruizhe Chen, Keqin Chen, Xionghui Chen, Zesen Cheng, Lianghao Deng, Wei Ding, Chang Gao, Chunjiang Ge, Wenbin Ge, Zhi-fang Guo, Qidong Huang, Jie Huang, Fei Huang, Binyuan Hui, Shutong Jiang, Zhaohai Li, Mingsheng Li, and 45 others. 2025b. *Qwen3-vl technical report*. *Preprint*, arXiv:2511.21631.

Shuai Bai, Keqin Chen, Xuejing Liu, Jialin Wang, Wen-bin Ge, Sibo Song, Kai Dang, Peng Wang, Shijie Wang, Jun Tang, and 1 others. 2025c. *Qwen2.5-vl technical report*. *arXiv preprint arXiv:2502.13923*.

Weikang Bai, Yongkun Du, Yuchen Su, Yazhen Xie, and Zhiheng Chen. 2025d. Complex mathematical expression recognition: Benchmark, large-scale dataset and strong baseline. *arXiv preprint arXiv:2512.13731*.

Lukas Blecher, Guillem Cucurull, Thomas Scialom, and Robert Stojnic. 2023. Nougat: Neural optical understanding for academic documents. *arXiv preprint arXiv:2308.13418*.

Guiming Hardy Chen, Shunian Chen, Ziche Liu, Feng Jiang, and Benyou Wang. 2024. Humans or llms as the judge? a study on judgement biases. *arXiv preprint arXiv:2402.10669*.

Xinyan Chen, Renrui Zhang, Dongzhi Jiang, Aojun Zhou, Shilin Yan, Weifeng Lin, and Hongsheng Li. 2025a. Mint-cot: Enabling interleaved visual tokens in mathematical chain-of-thought reasoning. *arXiv preprint arXiv:2506.05331*.

Zui Chen, Tianqiao Liu, Mi Tian, Qing Tong, Weiqi Luo, and Zitao Liu. 2025b. Advancing mathematical reasoning in language models: The impact of problem-solving data, data synthesis methods, and training stages. *arXiv preprint arXiv:2501.14002*.

Gheorghe Comanici, Eric Bieber, Mike Schaeckermann, Ice Pasupat, Noveen Sachdeva, Inderjit Dhillon, Marcel Blistein, Ori Ram, Dan Zhang, Evan Rosen, and 1 others. 2025. Gemini 2.5: Pushing the frontier with advanced reasoning, multimodality, long context, and next generation agentic capabilities. *arXiv preprint arXiv:2507.06261*.

Cheng Cui, Ting Sun, Suyin Liang, Tingquan Gao, Zelun Zhang, Jiaxuan Liu, Xueqing Wang, Changda Zhou, Hongen Liu, Manhui Lin, and 1 others. 2025. Paddleocr-vl: Boosting multilingual document parsing via a 0.9 b ultra-compact vision-language model. *arXiv preprint arXiv:2510.14528*.

Jun Feng, Zixin Wang, Zhentao Zhang, Yue Guo, Zhihan Zhou, Xiuyi Chen, Zhenyang Li, and Dawei Yin. 2025. Mathreal: We keep it real! a real scene benchmark for evaluating math reasoning in multimodal large language models. *arXiv preprint arXiv:2508.06009*.

Ling Fu, Zhebin Kuang, Jiajun Song, Mingxin Huang, Biao Yang, Yuzhe Li, Linghao Zhu, Qidi Luo, Xinyu Wang, Hao Lu, and 1 others. 2024. Ocrbench v2: An improved benchmark for evaluating large multimodal models on visual text localization and reasoning. *arXiv preprint arXiv:2501.00321*.

Hariyanto, Francisca Xaveria Diah Kristianingsih, and Rizqona Maharani. 2025. Artificial intelligence in adaptive education: a systematic review of techniques for personalized learning. *Discover Education*, 4(1):458.

Ahmed Heakl, Muhammad Abdullah Sohail, Mukul Ranjan, Rania Elbadry, Ghazi Shazan Ahmad, Mohamed El-Geish, Omar Maher, Zhiqiang Shen, Fahad Shahbaz Khan, and Salman Khan. 2025. Kitab-bench: A comprehensive multi-domain benchmark for arabic ocr and document understanding. In *Findings of the Association for Computational Linguistics: ACL 2025*, pages 22006–22024.

Pius Horn and Janis Keuper. 2025. Benchmarking document parsers on mathematical formula extraction from pdfs. *arXiv preprint arXiv:2512.09874*.

Anwen Hu, Haiyang Xu, Jiabo Ye, Ming Yan, Liang Zhang, Bo Zhang, Ji Zhang, Qin Jin, Fei Huang, and Jingren Zhou. 2024. mplug-docowl 1.5: Unified structure learning for ocr-free document understanding. In *Findings of the Association for Computational Linguistics: EMNLP 2024*, pages 3096–3120.

Aaron Hurst, Adam Lerer, Adam P Goucher, Adam Perelman, Aditya Ramesh, Aidan Clark, AJ Ostrow, Akila Welihinda, Alan Hayes, Alec Radford, and 1 others. 2024. Gpt-4o system card. *arXiv preprint arXiv:2410.21276*.

Guillaume Jaume, Hazim Kemal Ekenel, and Jean-Philippe Thiran. 2019. Funsd: A dataset for form understanding in noisy scanned documents. In *2019 International Conference on Document Analysis and Recognition Workshops (ICDARW)*, volume 2, pages 1–6. IEEE.

Daesik Kim, Seonhoon Kim, and Nojun Kwak. 2019. Textbook question answering with multi-modal context graph understanding and self-supervised open-set comprehension. In *Proceedings of the 57th Annual Meeting of the Association for Computational Linguistics*, pages 3568–3584.

Bo Li, Yuanhan Zhang, Dong Guo, Renrui Zhang, Feng Li, Hao Zhang, Kaichen Zhang, Peiyuan Zhang, Yanwei Li, Ziwei Liu, and 1 others. 2024. Llava-onevision: Easy visual task transfer. *arXiv preprint arXiv:2408.03326*.

Minghao Li, Yiheng Xu, Lei Cui, Shaohan Huang, Furu Wei, Zhoujun Li, and Ming Zhou. 2020a. Docbank: A benchmark dataset for document layout analysis. *arXiv preprint arXiv:2006.01038*.

Zhe Li, Lianwen Jin, Songxuan Lai, and Yecheng Zhu. 2020b. Improving attention-based handwritten mathematical expression recognition with scale augmentation and drop attention. In *2020 17th International Conference on Frontiers in Handwriting Recognition (ICFHR)*, pages 175–180. IEEE.

Aixin Liu, Aoxue Mei, Bangcai Lin, Bing Xue, Bingxuan Wang, Bingzheng Xu, Bochao Wu, Bowei Zhang, Chaofan Lin, Chen Dong, and 1 others. 2025a. Deepseek-v3. 2: Pushing the frontier of open large language models. *arXiv preprint arXiv:2512.02556*.

Wentao Liu, Qianjun Pan, Yi Zhang, Zhuo Liu, Ji Wu, Jie Zhou, Aimin Zhou, Qin Chen, Bo Jiang, and Liang He. 2025b. Cmm-math: A chinese multimodal math dataset to evaluate and enhance the mathematics reasoning of large multimodal models. In *Proceedings of the 33rd ACM International Conference on Multimedia*, pages 12585–12591.

Yuliang Liu, Zhang Li, Mingxin Huang, Biao Yang, Wenwen Yu, Chunyuan Li, Xu-Cheng Yin, Cheng-Lin Liu, Lianwen Jin, and Xiang Bai. 2024. Ocr-bench: on the hidden mystery of ocr in large multimodal models. *Science China Information Sciences*, 67(12):220102.

Pan Lu, Hritik Bansal, Tony Xia, Jiacheng Liu, Chunyuan Li, Hannaneh Hajishirzi, Hao Cheng, Kai-Wei Chang, Michel Galley, and Jianfeng Gao. 2023. Mathvista: Evaluating mathematical reasoning of foundation models in visual contexts. *arXiv preprint arXiv:2310.02255*.

Yubo Ma, Yuhang Zang, Liangyu Chen, Meiqi Chen, Yizhu Jiao, Xinze Li, Xinyuan Lu, Ziyu Liu, Yan Ma, Xiaoyi Dong, and 1 others. 2024. Mmlongbench-doc: Benchmarking long-context document understanding with visualizations. *Advances in Neural Information Processing Systems*, 37:95963–96010.

Minesh Mathew, Dimosthenis Karatzas, and CV Jawahar. 2021. Docvqa: A dataset for vqa on document images. In *Proceedings of the IEEE/CVF winter conference on applications of computer vision*, pages 2200–2209.

Lingchen Meng, Jianwei Yang, Rui Tian, Xiyang Dai, Zuxuan Wu, Jianfeng Gao, and Yu-Gang Jiang. 2024. Deepstack: Deeply stacking visual tokens is surprisingly simple and effective for lmms. *Advances in Neural Information Processing Systems*, 37:23464–23487.

Junbo Niu, Zheng Liu, Zhuangcheng Gu, Bin Wang, Linke Ouyang, Zhiyuan Zhao, Tao Chu, Tianyao He, Fan Wu, Qintong Zhang, and 1 others. 2025. Mineru2. 5: A decoupled vision-language model for efficient high-resolution document parsing. *arXiv preprint arXiv:2509.22186*.

Linke Ouyang, Yuan Qu, Hongbin Zhou, Jiawei Zhu, Rui Zhang, Qunshu Lin, Bin Wang, Zhiyuan Zhao, Man Jiang, Xiaomeng Zhao, and 1 others. 2025. Omnidocbench: Benchmarking diverse pdf document parsing with comprehensive annotations. In *Proceedings of the Computer Vision and Pattern Recognition Conference*, pages 24838–24848.

Hanoona Rasheed, Muhammad Maaz, Sahal Shaji, Abdela Rahman Shaker, Salman Khan, Hisham Cholakkal, Rao M Anwer, Eric Xing, Ming-Hsuan Yang, and Fahad S Khan. 2024. Glamm: Pixel grounding large multimodal model. In *Proceedings of the IEEE/CVF Conference on Computer Vision and Pattern Recognition*, pages 13009–13018.

An-Lan Wang, Jingqun Tang, Lei Liao, Hao Feng, Qi Liu, Xiang Fei, Jinghui Lu, Han Wang, Hao Liu, Yuliang Liu, and 1 others. 2025. Wilddoc: How far are we from achieving comprehensive and robust document understanding in the wild? In *Proceedings of the 2025 Conference on Empirical Methods in Natural Language Processing*, pages 23002–23012.

Haoran Wei, Yaofeng Sun, and Yukun Li. 2025. Deepseek-ocr: Contexts optical compression. *arXiv preprint arXiv:2510.18234*.

Yibo Yan, Shen Wang, Jiahao Huo, Philip S Yu, Xuming Hu, and Qingsong Wen. 2025. Mathagent: Leveraging a mixture-of-math-agent framework for real-world multimodal mathematical error detection. *arXiv preprint arXiv:2503.18132*.

Zhibo Yang, Jun Tang, Zhaohai Li, Pengfei Wang, Jianqiang Wan, Humen Zhong, Xuejing Liu, Mingkun Yang, Peng Wang, Shuai Bai, and 1 others. 2025. Cc-ocr: A comprehensive and challenging ocr benchmark for evaluating large multimodal models in literacy. In *Proceedings of the IEEE/CVF International Conference on Computer Vision*, pages 21744–21754.

Maoyuan Ye, Jing Zhang, Juhua Liu, Bo Du, and Dacheng Tao. 2025. Logicocr: Do your large multimodal models excel at logical reasoning on text-rich images? *arXiv preprint arXiv:2505.12307*.

Renrui Zhang, Dongzhi Jiang, Yichi Zhang, Haokun Lin, Ziyu Guo, Pengshuo Qiu, Aojun Zhou, Pan Lu, Kai-Wei Chang, Yu Qiao, and 1 others. 2024. Mathverse: Does your multi-modal llm truly see the diagrams in visual math problems? In *European Conference on Computer Vision*, pages 169–186. Springer.

Xu Zhong, Elaheh ShafieiBavani, and Antonio Jimeno Yepes. 2020. Image-based table recognition: data, model, and evaluation. In *European conference on computer vision*, pages 564–580. Springer.

Xu Zhong, Jianbin Tang, and Antonio Jimeno Yepes. 2019. Publaynet: largest dataset ever for document layout analysis. In *2019 International conference on document analysis and recognition (ICDAR)*, pages 1015–1022. IEEE.

Yinan Zhou, Yuxin Chen, Haokun Lin, Yichen Wu, Shuyu Yang, Zhongang Qi, Chen Ma, and Li Zhu. 2025. Dogr: Towards versatile visual document grounding and referring. In *Proceedings of the IEEE/CVF International Conference on Computer Vision*, pages 3596–3606.

Jinguo Zhu, Weiyun Wang, Zhe Chen, Zhaoyang Liu, Shenglong Ye, Lixin Gu, Hao Tian, Yuchen Duan, Weijie Su, Jie Shao, and 1 others. 2025. Internvl3: Exploring advanced training and test-time recipes for open-source multimodal models. *arXiv preprint arXiv:2504.10479*.

A Appendix

A.1 The example of dataset

In this section, we present representative examples from the MathDoc dataset, illustrating unrecognizable questions in Figure 9.

A.2 The fairness of LLM as judge

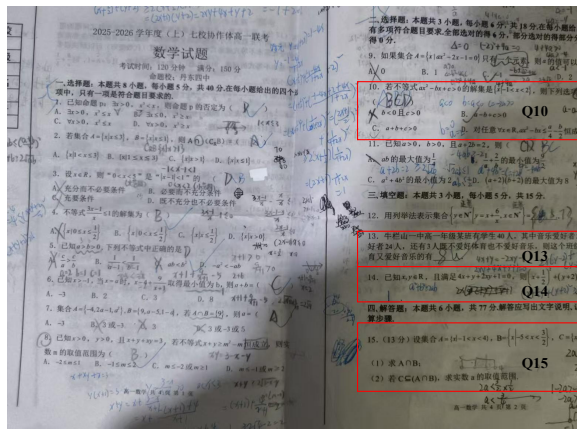
We note that our evaluation relies on Large Language Model as automatic judge. Rather than claiming absolute objectivity, we aim to demonstrate that under our constrained evaluation protocol, the judge exhibits consistent and interpretable behavior.

First, for image-based verification, the judge is restricted to assessing semantic consistency under a fixed instruction, rather than subjective visual quality. We therefore avoid pixel-level metrics such as IoU, which are highly sensitive to common layout variations in real-world documents and may not reliably reflect semantic validity. As shown in Figure 10, two images with moderate IoU can still be semantically equivalent and are correctly assigned a high score by the LLM-based judge. In contrast, Figure 11 presents a visually similar prediction that omits critical semantic elements and is accordingly penalized.

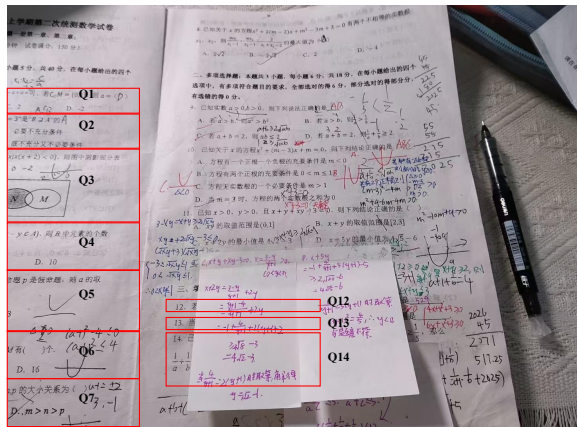
Second, at the text level, the judge is designed to tolerate common OCR-induced noise while preserving strict semantic alignment between the predicted and ground-truth questions. Figure 12 provides a representative matching example.

A.3 Prompt Details

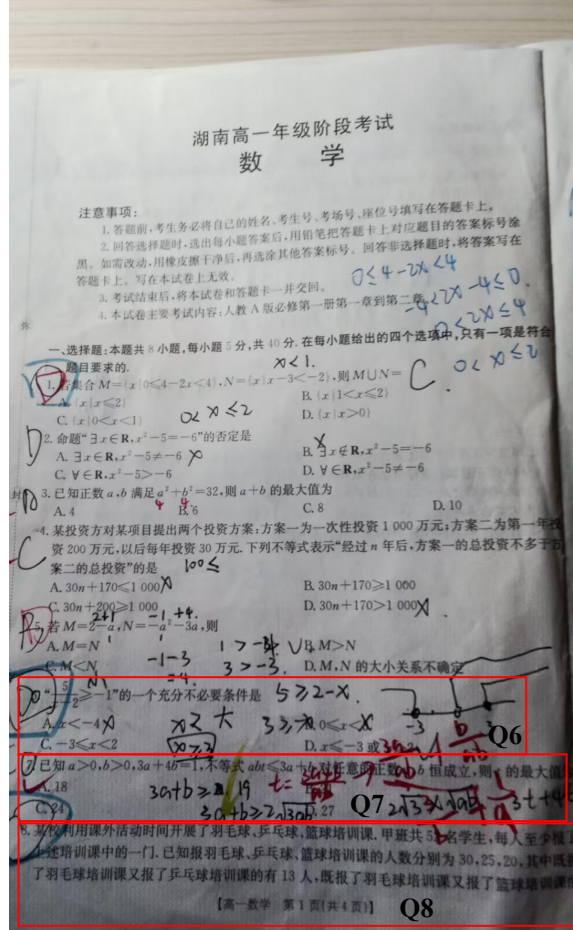
In this section, we detail the prompts used in our evaluation pipeline. For readability, we present the English version of the prompt. The experiments are conducted using the original Chinese prompt, which is semantically equivalent. Specifically, we describe: (i) the prompt used to guide a language model in identifying the start and end indices of the predicted text spans within the generated output (Figure 14); (ii) the prompt employed in an **MLLM-as-a-judge** setting to assess semantic similarity between ground-truth figures and model-predicted cropped images (Figure 13); and (iii) the prompt provided to **MLLMs** for document-level information extraction (Figure 15).



(a)



(b)



(c)

Figure 9: Examples of three categories of unrecognizable cases defined in our work: (i) heavy handwriting occlusions and corrections in critical text regions; (ii) physical obstructions (e.g., stains and wrinkles); and (iii) compromised document integrity, such as incomplete questions or folded pages. Unrecognizable question regions are highlighted with red bounding boxes, as these degradations remove critical semantic information and violate the legibility constraints, thereby marked as [unrecognizable].

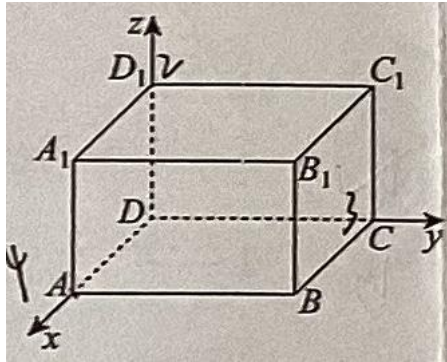


Image1(GT)

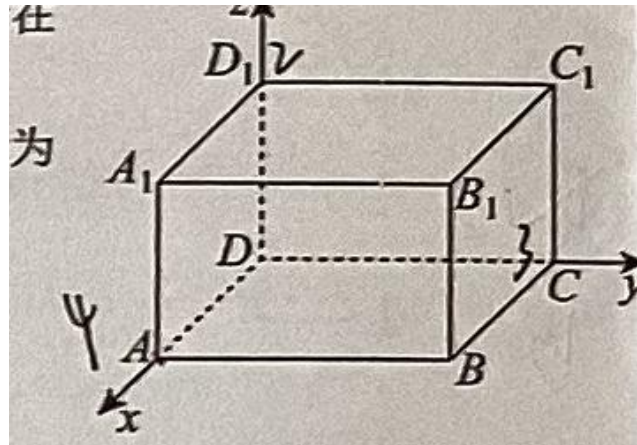


Image2(Pred)

Score: 1.0

Justification:

Completeness Check (Critical): The extracted image (Image 2) is a perfect, pixel-for-pixel match of the ground truth image (Image 1). All critical semantic information is preserved without any loss.

Textual Content: All labels (A, B, C, D, A₁, B₁, C₁, D₁, x, y, z) are fully visible and legible.

Graphical Elements: The entire 3D cube structure, including all vertices, edges (both solid and dashed), and the coordinate axes with their directional arrows, is completely intact. No vertices or edges are missing.

Redundancy Check (Secondary): The extracted image contains no excessive irrelevant background or whitespace. It is tightly cropped around the figure itself, which is ideal for this task as it focuses solely on the semantic content without introducing distractions.

Based on the scoring criteria, since Image 2 fully preserves all semantic information from Image 1 with no flaws, it falls into the 0.9 – 1.0 (Perfect / Excellent) category. The score is therefore 1.0.

Figure 10: An example of LLM-based image semantic similarity evaluation

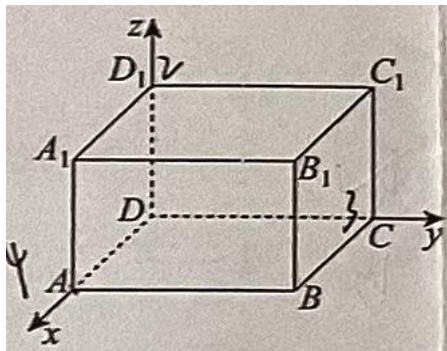


Image1(GT)

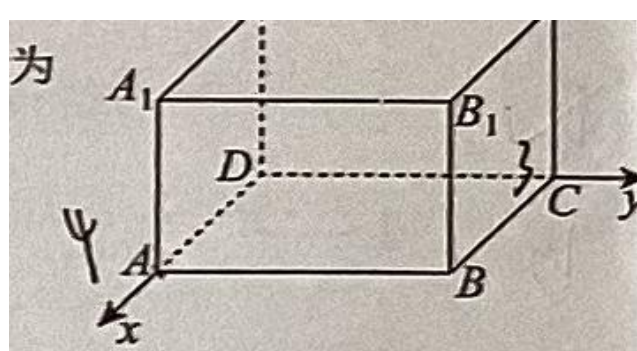


Image2(Pred)

Score: 0.55

Justification:

Critical semantic information is missing: the vertex label "D₁" is completely cropped out. In mathematical diagrams, vertex labels are essential structural components; their loss prevents faithful reconstruction of the problem without inference, which is strictly prohibited by the evaluation protocol. This constitutes a critical failure under the "Unusable" category (score < 0.6).

The extraneous background characters do not affect readability and are not penalized.

Figure 11: A failure case correctly identified by the LLM-based semantic judge

GT text	Pred text
<p>9. Given the universal set $U = A \cup B$, where $A = \{1, 3, 4\}$, $B = \{x \in \mathbb{N} \mid \frac{6}{x} \in \mathbb{N}\}$, then ()</p> <p>A. $2 \in B$ B. $A \cap B = \{1, 3\}$ C. The number of elements in U is 5 D. Let $C = \{x \mid x \text{ is a prime number}\}$, then the number of subsets of $C \cap B$ is 8</p> <p>GT_start GT_end</p>	<p>9. Given the universal set $U = A \cup B$, where $A = \{1, 3, 4\}$, $B = \{x \in \mathbb{N} \mid \frac{6}{x} \in \mathbb{N}\}$, then ()</p> <p>A. $2 \in B$ B. $A \cap B = \{1, 3\}$ C. The number of elements in U is 5 D. Let $C = \{x \mid x \text{ is a prime number}\}$, then the number of subsets of $C \cap B$ is 8</p> <p>Pred_start Pred_end</p>
<p>10. Given that the solution set of the inequality $ax^2 + bx + c > 0$ is $\{x \mid -2 < x < 3\}$, which of the following statements are correct? ()</p> <p>A. $a > 0$ B. $a + b + c > 0$ C. The solution set of the inequality $ax^2 + bx + a < 0$ is $\{x \mid -\frac{1}{3} < x < \frac{1}{2}\}$ D. When $c = 6$, the solution set of the inequality $\frac{(x+a)(x+b)}{x+c} > 0$ is $\{x \mid -6 < x < -1 \text{ or } x > 1\}$</p>	<p>10. the inequality $ax^2 + c > 0$ is $\{x \mid x < 3\}$, which of are correct? ()</p> <p>A. $a > 0$ B. $a + b + c > 0$ C. of the inequality $cx^2 + bx + a < 0$ is $\{x \mid -\frac{1}{3} < x < \frac{1}{2}\}$ D. When $c = 6$, the solution set of the inequality $\frac{(x+a)(x+c)}{x+b} > 0$ is $\{x < -1 \text{ or } x > 1\}$</p>

Figure 12: Illustration of dual-anchor semantic alignment between ground-truth and predicted text. The left hand-side two questions are all from GT, the right hand-side two are all from Pred text stream.

Role. You are a *Visual Semantic Completeness Evaluator* with expertise in the structured assessment of mathematical documents. Your objective is to evaluate the semantic completeness of an *Extracted Image* (Image 2) relative to its corresponding *Ground Truth Image* (Image 1).

Task. Given a pair of images, assess whether Image 2 faithfully preserves all semantic information present in Image 1. This includes textual content, mathematical expressions, and graphical elements.

1. Evaluation Procedure

- **Completeness Check (Critical).** Carefully compare Image 2 against Image 1 and determine whether any critical semantic information is missing. This includes, but is not limited to: truncated text, missing vertices or edges in geometric figures, and blurred or omitted superscripts/subscripts in formulas.
- **Redundancy Check (Secondary).** Examine whether Image 2 contains excessive irrelevant background or whitespace. Additional whitespace is acceptable as long as it does not interfere with content readability or interpretation.

2. Scoring Criteria

- **0.9 – 1.0 (Perfect / Excellent).** Image 2 fully preserves all semantic information from Image 1.
- **0.6 – 0.8 (Pass / Minor Flaws).** The semantic content is fundamentally complete with negligible defects.
- **0.0 – 0.59 (Unusable).** Any semantic or structural loss that prevents full reconstruction of the original problem meaning.

Figure 13: Prompt used for evaluating the visual similarity of extracted mathematical document images.

Role. You are an *OCR Text Alignment Expert*. Your objective is to map structured questions from the *Ground Truth (GT)* to their *physical boundaries* within the noisy *Predicted Text (Pred)*.

Task. Establish a correspondence between clean GT questions and noisy Pred content. For each GT question, identify the exact `pred_start_snippet` and `pred_end_snippet` in Pred.

1. Core Principles

- **Monotonicity (Strict Order).** Question order in Pred must strictly follow GT. The start of Question N must appear *after* the end of Question $N - 1$. No backtracking or overlap is allowed.
- **Verbatim Extraction.** `pred_start_snippet` and `pred_end_snippet` must be copied *exactly* from Pred, preserving all OCR errors, garbled characters, and missing punctuation. Do *not* normalize or correct the text.
- **Physical Truncation Strategy.** Do not struggle to search for a semantic ending of Question N . Instead, if the end can not be found, try to locate the start of Question $N+1$. The end of Question N is defined as the text segment immediately preceding it.
- **Robustness to Failure.** If Question N cannot be matched due to severe noise or missing content, return empty strings and *immediately proceed* to align Question $N+1$. Maximize the number of aligned questions.

2. Alignment Strategy

For each GT question:

- **Locate Start.** Identify the question beginning in Pred using *semantic similarity*. Prioritize topic-level matching (e.g., *Complex Numbers, Vectors*) even when mathematical expressions are distorted (e.g., $z = 1 + i$ vs. $z = 2/(1 + i)$).
- **Ignore Status Tags.** Skip metadata or preprocessing tags (e.g., `[Format Normal]`) and begin extraction from the actual question content or index.
- **Locate End.** Identify the start of Question $N+1$. The end of Question N is the text segment strictly before it. Garbled text is acceptable as long as it lies within the physical boundary.

3. Output Schema

Return a *pure JSON list* containing objects with the following fields:

```
{question_id, gt_start_snippet, gt_end_snippet, pred_start_snippet, pred_end_snippet, pred_answer}
```

Extract answers as concise values (e.g., A , 3 , `[Answer: X]`). Return empty strings if no answer is found. Do *not* extract full question text.

4. Few-Shot

- **Distorted Mathematics.** GT: $z=2/(1+i)$; Pred: $z=1+i$. Match based on the shared semantic topic.
- **Missing Index.** GT: $18.$ Function ...; Pred: (17pts) Function Match using semantic context despite index loss.
- **Unrecognizable Content.** If the GT marks a question as `[Unrecognizable]`, inspect the corresponding section in Pred. Consider the question *successfully aligned* if the Pred content is either: 1) **Empty** (null string), or 2) Explicitly contains **unrecognizability indicators** (e.g., “unrecognizable”, “illegible”, or failure tokens). In these cases, extract the empty string or the specific indicator as the snippet and proceed to the next question.

Figure 14: Full prompt used for OCR question-to-text boundary alignment under severe noise.

Role. You are a *Strict Document Structure Analysis Specialist*. Your objective is to accurately transcribe the printed structure of exam papers without performing mathematical problem-solving or speculative completion.

Global Constraints: (1) **No Subjective Solving:** Do not solve mathematical problems or reason about correctness. (2) **No Hallucination:** If printed text is occluded or missing, do not guess or complete it. (3) **Strict Mode Switching:** Apply transcription rules strictly according to the question type defined below.

Workflow: Execute the following logic pipeline sequentially for each detected question region.

Step 1: Legibility & Integrity Check.

Condition: If any critical printed information (question index, stem content, or specific options) is blurred, occluded, or missing due to folding, stains, or damage.

Action: Immediately output:

```
[ID]. [Unrecognizable]
```

and terminate processing for this question. Do not attempt to repair or infer the text.

Step 2: Question Mode Classification & Transcription

Classify the question into one of the following modes and apply the corresponding strict rules.

Mode A: Subjective Questions (Calculation / Proof).

Characteristics: High point value (e.g., >10 points), sub-questions such as (1)(2), or directives like “Prove” or “Solve”.
Rules: Transcribe the printed question stem only. Strictly ignore all handwritten content.

Mode B: Objective Questions (Multiple Choice / Fill-in-the-Blank). *Characteristics:* Presence of options (A/B/C/D) or underline placeholders.

Rules:

- Transcribe all printed options (A, B, C, D) completely.
- **Answer Extraction:** If a handwritten mark (e.g., a tick or letter) is explicitly visible, append [Answer: X] at the end. If the answer area is blank, output printed text only.
- **Prohibition:** Do not infer answers based on internal knowledge. If no handwriting is present, do not generate an answer tag.

Step 3: Figure Extraction

Target: Computer-generated diagrams only (e.g., geometric figures or function plots).

Action: Append an image marker after the question stem using normalized coordinates:

```
<!-- Image (x1, y1, x2, y2) -->
```

where coordinates are normalized to the range [0, 1000].

Few-Shot Demonstrations (Illustrative)

Example 1: Objective (Answered).

Input: Question 5 with handwritten “C” marked in the answer bracket.

Output:

Let $M = \{1, 2\}$, $N = \{2, 3\}$, then $M \cup N = ()$ [Answer: C]
A. {1} B. {2} C. {1, 2, 3} D. {3}

Example 2: Objective (Unanswered).

Input: Question 6 with an empty answer bracket.

Output:

Which of the following functions is an even function? ()
A. $y = x$ B. $y = x^2$ C. $y = \sin x$ D. $y = e^x$

(No answer tag is generated.)

Example 3: Subjective (Handwriting Ignored).

Input: Question 17 (10 points) with handwritten formulas covering whitespace.

Output:

(10 points) As shown in the figure...
(1) Prove that...
<!-- Image (50, 60, 150, 160) -->

Example 4: Illegible Input (Refusal).

Input: Question 8 partially covered by a page fold.

Output:

```
[Unrecognizable]
```

Figure 15: Prompt specifying strict rules for document structure analysis and transcription of exam papers.